

Species Abundance Distribution and Species Accumulation Curve: A General Framework and Results

Cheuk Ting LI

Department of Information Engineering,
The Chinese University of Hong Kong,
Hong Kong SAR of China.

ctli@ie.cuhk.edu.hk

Kim-Hung LI

Asian Cities Research Centre Ltd.,
Hong Kong SAR of China.

khli@acrc.hk

September 21, 2021

Abstract

We build a general framework which establishes a one-to-one correspondence between species abundance distribution (SAD) and species accumulation curve (SAC). The appearance rates of the species and the appearance times of individuals of each species are modeled as Poisson processes. The number of species can be finite or infinite. Hill numbers are extended to the framework. We introduce a linear derivative ratio family of models, LDR_1 , of which the ratio of the first and the second derivatives of the expected SAC is a linear function. A D1/D2 plot is proposed to detect this linear pattern in the data. The SAD of LDR_1 is the Engen's extended negative binomial distribution, and the SAC encompasses several

popular parametric forms including the power law. Family LDR_1 is extended in two ways: LDR_2 which allows species with zero detection probability, and RDR_1 where the derivative ratio is a rational function. We also consider the scenario where we record only a few leading appearance times of each species. We show how maximum likelihood inference can be performed when only the empirical SAC is observed, and elucidate its advantages over the traditional curve-fitting method.

Keywords: Engen’s extended negative binomial distribution; Hill numbers; Power law; Rarefaction curve; Species-time relationship.

1 Introduction

Estimating the diversity of classes in a population is a problem encountered in many fields. We may be interested in the diversity of words a person know from his/her writings [Efron and Thisted, 1976], the illegal immigrants from the apprehension records [Böhning and Schön, 2005], the distinct attributes in a database [Haas et al., 1995, Deolalikar and Laffitte, 2016], or the distinct responses to a crowdsourcing query [Trushkowsky et al., 2012]. Among different applications, species abundance is the one that receives most attention. For this reason, it is chosen as the theme of this paper with the understanding that the proposed framework and methods are applicable in other applications as well.

Understanding the species abundance in an ecological community has long been an important task for ecologists. Such knowledge is paramount in conservation planning and biodiversity management [Matthews and Whittaker, 2015]. An exhaustive species inventory is too labor and resource intensive to be practical. Information about species abundance can thus be acquired mainly through a survey.

Let $N = (N_0, N_1, \dots)$ where N_k is the number of species in a community that are represented exactly k times in a survey. We do not observe the whole N , but $\tilde{N} = (N_1, N_2, \dots)$ which is the zero-truncated N . In other words, we do not know how many species are not seen in the survey. We call the vector \tilde{N} , the frequency of frequencies (FoF) [Good, 1953].

A plethora of species abundance models have been proposed for \tilde{N} . Comprehensive review of the field can be found in Matthews and Whittaker [2014]. A typical assumption in purely statistical models is

$$\tilde{N} | N_+ \sim \text{Multinomial}(N_+, p), \quad (1)$$

where $N_+ = \sum_{k=1}^{\infty} N_k$ is the total number of recorded species, and $p = (p_1, p_2, \dots)$ is a probability vector, such that p_k is the probability for a randomly selected recorded species to be observed k times in the study for $k = 1, 2, \dots$. We call this vector p , the species abundance distribution (SAD). Species accumulation curve (SAC) is another tool in the analysis of species abundance data. The survey is viewed as a data-collection process in which more and more sampling effort is devoted. SAC is the number of recorded species expressed as a function of the amount of sampling effort.

Despite the different emphases of SAD and SAC, the two approaches have an overlapped target: Estimating D , the total number of species in the community. For SAD, it means estimating N_0 , the number of unseen species as $D = N_0 + N_+$. For SAC, D is the total number of seen species when the sampling effort is unlimited.

As SAD depends largely on the sampling effort, it is necessary to include sampling effort explicitly in the model in order to make comparison of different SADs possible. This addition establishes a link between SAD and SAC. Sampling effort can be of continuous type, such as the area of land or the volume of water sampled, or the duration of the survey. Discrete type sampling effort can be the sample size. To emphasize the sampling effort considered, the SAC is called species-time curve, species-area curve, or species-sample-size curve when the sampling effort is time, area, or sample size respectively. Species-area curve has been studied extensively in the literature. Review of it can be found in Tjørve [2003, 2009], Dengler [2009] and Williams et al. [2009]. In this paper, we use time as the measure of sampling effort. We consider the vector N to be a function of the time t , denoted as $N(t)$. Notations N_k , \tilde{N} , N_+ , p and p_k are likewise denoted as $N_k(t)$, $\tilde{N}(t)$, $N_+(t)$, $p(t)$ and $p_k(t)$ respectively. Because of the great similarity of the species-time relationship and species-area relationship [Preston, 1960, Magurran, 2007], time and area are treated as if they are interchangeable in this paper. When SAC is species-area curve, we refer to the Type I species-area curve [Scheiner, 2003], where the areas sampled are nested (smaller areas are included in larger areas),

resulting in a curve that is always nondecreasing. Throughout the paper, we assume without loss of generality that the survey starts at time 0 and ends at time $t_0 > 0$.

Finite D is commonplace in SAD approach although no consensus has been reached. Empirically, log-series distribution, a SAD that assumes infinite D , is one of the most successful models. Many SACs do not have asymptote. It is common that the number of rare species is large, and shows no sign to decrease. In Bayesian nonparametric approach in genomic diversity study, Poisson-Dirichlet process which assumes infinite D is used (see for example Lijoi, Mena, and Prünster [2007]). In reality, the existence of transient species (species which are observed erratically and infrequently [Novotny and Basset, 2000]), and the error in the species identification process (a well-known example is the missequencing in pyrosequencing of DNA (see for example Dickie [2010]) are continual sources of rare species making the species number larger than expected. For the above reasons, it is better to allow infinite D in the framework.

An extreme kind of rare species is species with zero detection probability. We call such species, zero-probability species, and all other species, positive-rate species. Zero-probability species can either be seen only once or unseen in a survey. If there are finite number of zero-probability species, the probability of observing any of them is zero. Therefore, if zero-probability species can be observed in a study, there must be an infinite number of them.

In this paper, we propose in Section 2 a new model for the sampling process, called the mixed Poisson partition process. It can handle the case where D is finite or infinite, and allows existence of zero-probability species. The framework models all observations in the study period. Once all parameters in the framework are estimated, we can make inference on different characteristics of the population, say the SAD at any fixed time, the Hill numbers, or the expected future data. We study $\tilde{N}(t)$ in Section 3. In Section 4, we consider the expected species accumulation curve (ESAC). It is shown that there is one-to-one correspondence between a mixed Poisson partition process and an ESAC which is a Bernstein function that passes through the origin. In Section 5, we introduce LDR_1 , a parametric family of ESAC. The SAD of LDR_1 is the Engen's extended negative binomial distribution. This family has an attractive property that the ratio of the first and the second derivatives of the ESAC is a linear function of t .

A D1/D2 plot is proposed to detect this linear relation. We extend LDR_1 to LDR_2 which allows zero-probability species. In Section 6, LDR_1 is generalized so that the derivative ratio is a rational polynomial instead of a linear function of t . Three real data are analyzed in Section 7 to demonstrate the applications of the proposed models. In Section 8, we propose and study a design where only a few leading appearance times of each species are recorded. In Section 9, we consider the maximum likelihood approach on the empirical SAC. We give a conclusion in Section 10.

2 Mixed Poisson Partition Process

We model the observations in a species abundance survey by a stochastic process called mixed Poisson partition process where rates of the species follows a Poisson process.

Definition: (Mixed Poisson partition process) A mixed Poisson partition process, G , is characterized by a species intensity measure ν , which is a measure over $\mathbb{R}_{\geq 0}$, the set of all nonnegative real numbers, satisfying

$$\int_0^{\infty} \min\{1, \lambda^{-1}\} \nu(d\lambda) < \infty. \quad (2)$$

The definition of a mixed Poisson partition process consists of three steps:

1. (Generation of positive rates of species) Given ν , define $\tilde{\nu}$ to be a measure over $\mathbb{R}_{>0}$ ($\mathbb{R}_{>0}$ is the set of positive real numbers) by $\tilde{\nu}(d\lambda) = \nu(d\lambda)/\lambda$, (i.e., $d\tilde{\nu}/d\nu = 1/\lambda$ for $\lambda > 0$). Generate $\lambda_1, \lambda_2, \dots$ (a finite or countably infinite sequence) according to a Poisson process with intensity measure $\tilde{\nu}$.
2. (Generation of individuals of positive-rate species) For each λ_i in Step 1, we generate a realization η_i (independently across i) of a Poisson process with rate λ_i .
3. (Generation of individuals of zero-probability species) We generate a realization η_0 of a Poisson process with rate $\nu(\{0\})$, independent of η_1, η_2, \dots . This represents the times of appearance for all the zero-probability species.

Finally, we take $G = \{\eta_1, \eta_2, \dots\} \cup \eta_0$. For any $i \geq 1$, all points in η_i are from the same species, whereas each point in η_0 is from a different species (we use a slight abuse of notation to treat each point in η_0 as a point process with only one point).

Similar to Step 1, Zhou, Favaro, and Walker [2017] also considered the species to be generated according to a random process. However, their model does not involve time, and hence does not describe the species-time relationship. Although their model includes cases where D is infinite, it fails to handle zero-probability species.

Measures ν and $\tilde{\nu}$ may be finite or infinite. As the expected number of individuals seen in time interval $[0, t]$ is equal to $t\nu(\mathbb{R}_{\geq 0})$ (see (6) in Section 3), this expected value is finite when ν is finite. If $\tilde{\nu}$ is finite, the expected number of positive-rate species in the community is finite. From Step 3 in the definition, if $\nu(\{0\}) > 0$, there are infinite number of zero-probability species and they arrive at a constant rate. With probability one, D is finite if and only if $\nu(\{0\}) = 0$ and $\tilde{\nu}(\mathbb{R}_{>0}) < \infty$ (see (5) in Section 3). In such case, D follows a Poisson($\tilde{\nu}(\mathbb{R}_{>0})$) distribution. Measure $\tilde{\nu}$ specifies the distribution of the rates of positive-rate species. More precisely, $\tilde{\nu}([\lambda_0, \lambda_1])$ with $\lambda_0 > 0$ is the average number of species with rate in $[\lambda_0, \lambda_1]$. Measure ν specifies the distribution of the rates of the species of the individuals including those of the zero-probability species. More precisely, $\nu([\lambda_0, \lambda_1])$ is the average number of individuals (per unit time) belonging to species whose rates lie in $[\lambda_0, \lambda_1]$. Condition (2) is essential because it is equivalent to the finiteness of the ESAC (i.e. $E(N_+(t)) < \infty$ for any finite nonnegative t). A proof of it is given in Appendix B. Figure 1 illustrates the generation of the mixed Poisson partition process. An alternative equivalent definition that unifies the generation of individuals of zero-probability species and positive-rate species is given in Appendix A.

A special feature of the framework is that D is random and can be infinite with probability one. This change necessitates modification of biodiversity measures, among which Hill numbers are popular. When D is deterministic, Hill number of order q [Hill, 1973] for $q \geq 0$ and $q \neq 1$ is ${}^qD = \left(\sum_i (p_{\text{sp}}(i))^q \right)^{1/(1-q)}$ where $p_{\text{sp}}(i)$ is the relative abundance of species i in an assemblage (the number of individuals of species i divided by the total population). When $q = 1$, 1D is defined as $\lim_{q \rightarrow 1} {}^qD = \exp(-\sum_i p_{\text{sp}}(i) \log(p_{\text{sp}}(i)))$. Three important qD 's are ${}^0D (= D)$ (species richness), 1D (Shannon diversity), and 2D (inverse Simpson concentration).

Under our framework, each species correspond to a Poisson process, and the relative abundance of a species is its rate divided by the expected total rate, $\Lambda = \int \nu(d\lambda)$.

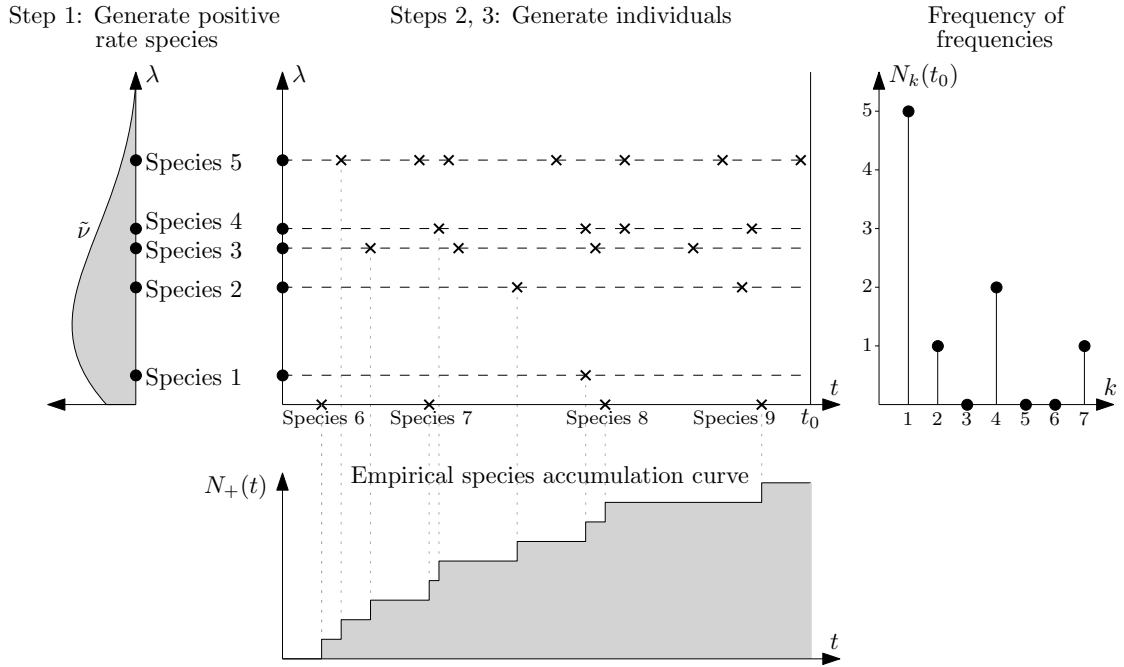


Figure 1: An illustration of the mixed Poisson partition process. In step 1, we generate the rates λ_i of the positive-rate species according to a Poisson process with intensity measure $\tilde{\nu}$. If $\tilde{\nu}(\mathbb{R}_{>0}) < \infty$, then this is equivalent to first generating n_{pos} , the number of positive-rate species according to $\text{Poisson}(\tilde{\nu}(\mathbb{R}_{>0}))$, and then generating a random sample $\lambda_1, \dots, \lambda_{n_{pos}}$ of size n_{pos} from the probability measure $\tilde{\nu}/\tilde{\nu}(\mathbb{R}_{>0})$. In step 2, we generate the individuals of species i according to a Poisson process with rate λ_i for $i = 1, \dots, n_{pos}$. In step 3, we generate the individuals of zero-probability species (species 6 to 9 in the figure) according to a Poisson process with rate $\nu(\{0\})$.

Reasonable modifications to the definition of Hill numbers are to replace $p_{\text{sp}}(i)$ with λ/Λ , where λ is the rate of a species, and to replace summation over species with integration with respect to the measure $\lambda^{-1}\nu$ so that the integral of λ/Λ is one. It works well when Λ is finite, but fails when Λ is infinite (i.e. ν is infinite). To fix the problem, we need a meaningful surrogate rate which fulfills two requirements: (i) the expected total rate is finite, and (ii) it approaches the true rate λ as a limit. For a species with rate λ , the density function of its first appearance time is $\lambda \exp(-\lambda t)$, which can be regarded as the instantaneous rate of its first appearance at time t . This rate approaches λ when t decreases to zero. The expected total instantaneous rate of first appearances over all species at time t is $\Lambda_t = \int \exp(-\lambda t) \nu(d\lambda)$ ($= E(N_1(t))/t$ from (3)) which is always finite for positive t . Replacing $p_{\text{sp}}(i)$ with $\lambda \exp(-\lambda t)/\Lambda_t$ and taking $t \rightarrow 0$, we define, the Hill numbers, ${}^qD_\nu$ with $q \geq 0$ and $q \neq 1$ for our framework as

$${}^qD_\nu = \lim_{t \rightarrow 0} \left(\Lambda_t^{-q} \int \lambda^{q-1} \exp(-\lambda q t) \nu(d\lambda) \right)^{1/(1-q)}.$$

We define ${}^1D_\nu$ as

$${}^1D_\nu = \lim_{q \rightarrow 1} {}^qD_\nu = \lim_{t \rightarrow 0} \Lambda_t \exp \left(-\frac{1}{\Lambda_t} \int (\log \lambda - \lambda t) \exp(-\lambda t) \nu(d\lambda) \right).$$

When Λ is finite,

$${}^qD_\nu = \begin{cases} \left(\Lambda^{-q} \int \lambda^{q-1} \nu(d\lambda) \right)^{1/(1-q)} & (q \geq 0, q \neq 1) \\ \Lambda \exp \left(-\frac{1}{\Lambda} \int \log(\lambda) \nu(d\lambda) \right) & (q = 1). \end{cases}$$

Diversity ${}^qD_\nu$ is non-increasing with respect to q . Unlike the classical Hill numbers, ${}^qD_\nu$ can be less than one. For instance, from (5), ${}^0D_\nu = E(D)$ which can be any nonnegative value. It can be proved that for any positive α , ${}^qD_\nu = \alpha ({}^qD_{\nu/\alpha})$, an analogue of the replication principle for Hill numbers.

3 Frequency of Frequencies

A sufficient statistic for a realization G of a mixed Poisson partition process in time interval $[0, t_0]$ is $\tilde{N}(t_0)$. It can be shown that for $k \geq 1$

$$E(N_k(t)) = \int \frac{(\lambda t)^k e^{-\lambda t}}{k!} \tilde{\nu}(d\lambda) + \mathbf{1}\{k = 1\} \nu(\{0\}) t = \int \frac{\lambda^{k-1} t^k e^{-\lambda t}}{k!} \nu(d\lambda), \quad (3)$$

$$E(N_+(t)) = \sum_{k=1}^{\infty} E(N_k(t)) = \int \frac{1 - e^{-\lambda t}}{\lambda} \nu(d\lambda), \quad (4)$$

$$E(D) = \lim_{t \rightarrow \infty} E(N_+(t)) = \lim_{t \rightarrow \infty} \int \frac{1 - e^{-\lambda t}}{\lambda} \nu(d\lambda) = \int \lambda^{-1} \nu(d\lambda), \quad (5)$$

where $\mathbf{1}\{\cdot\}$ is the indicator function (we use the convention that $0^0 = 1$). When $\nu(\{0\}) > 0$, $E(D)$ is infinite. Furthermore, all elements in $\{N_k(t)\}_{k \geq 1}$ are independent and each follows a Poisson distribution. The last expression in Equation (3) holds also when $k = 0$. Variable $N_+(t)$ is Poisson distributed, and so do D and $N_0(t)$ when their expected values are finite.

Let $S(t) = \sum_{k=1}^{\infty} k N_k(t)$ be the number of individuals observed before time t . Then

$$E(S(t)) = \sum_{k=1}^{\infty} k \int \frac{\lambda^{k-1} t^k \exp(-\lambda t)}{k!} \nu(d\lambda) = t \int \nu(d\lambda). \quad (6)$$

It is easy to see that model (1) is valid under the framework, and

$$p_k(t) = \frac{E(N_k(t))}{E(N_+(t))} = \frac{\int (k!)^{-1} \lambda^{k-1} t^k \exp(-\lambda t) \nu(d\lambda)}{\int \lambda^{-1} (1 - \exp(-\lambda t)) \nu(d\lambda)} \quad (k = 1, 2, \dots). \quad (7)$$

If $E(D)$ is finite, $\lim_{t \rightarrow \infty} p_k(t) = 0$ for any fixed k . Let $n_k(t_0)$ be the observed $N_k(t_0)$ for $k = 1, 2, \dots$ and $\tilde{n}(t_0) = \{n_k(t_0)\}_{k \geq 1}$. The joint probability mass function of $\tilde{N}(t_0)$ is

$$P(\tilde{N}(t_0) = \tilde{n}(t_0) \mid \nu) = \exp(-E(N_+(t_0))) \prod_{k=1}^{\infty} \frac{(E(N_k(t_0)))^{n_k(t_0)}}{n_k(t_0)!}.$$

In terms of the expected FoF, the log-likelihood function is

$$\log(\mathcal{L}(\{E(N_k(t_0))\}_{k \geq 1} \mid \tilde{n}(t_0))) = -E(N_+(t_0)) + \sum_{k=1}^{\infty} n_k(t_0) \log(E(N_k(t_0))). \quad (8)$$

In terms of $p(t_0)$ and $E(N_+(t_0))$, it is

$$\log(\mathcal{L}(p(t_0), E(N_+(t_0)) \mid \tilde{n}(t_0))) = -E(N_+(t_0)) + n_+(t_0) \log(E(N_+(t_0))) + \sum_{k=1}^{\infty} n_k(t_0) \log(p_k(t_0)).$$

If the unknown vector $p(t_0)$ and the quantity $E(N_+(t_0))$ are unrelated, the above log-likelihood function implies that the maximum likelihood estimator (MLE) of $p(t_0)$ is the conditional maximum likelihood estimator (conditional on the observed $n_+(t_0)$) for the multinomial distribution in (1). The MLE of $E(N_+(t_0))$ is $n_+(t_0)$.

4 Expected Species Accumulation Curve

The empirical SAC is $N_+(t)$. We call its expectation, expected SAC (ESAC), and denote it as $\psi(t)$. Condition (2) guarantees that $\psi(t)$ is finite for any finite t . From Equation (4),

$$\psi(t) = \int \frac{1 - \exp(-\lambda t)}{\lambda} \nu(d\lambda) = \nu(\{0\})t + \int (1 - \exp(-\lambda t)) \tilde{\nu}(d\lambda). \quad (9)$$

Hence, for $k = 1, 2, \dots$,

$$\psi^{(k)}(t) = \int (-\lambda)^{k-1} \exp(-\lambda t) \nu(d\lambda), \quad (10)$$

where $g^{(m)}(t)$ stands for the m -order derivative of function $g(t)$. From (10), $\psi(t)$ is a Bernstein function (a function $g(t)$ is a Bernstein function if it is a nonnegative real-valued function on $[0, \infty)$ such that $(-1)^k g^{(k)}(t) \leq 0$ for all positive integer k). In considering a restricted model, Boneh, Boneh, and Caron [1998] found that $(-1)^{k+1} \psi^{(k)}(t) \geq 0$ and called it, alternating copositivity. Every Bernstein function $g(t)$ with $g(0) = 0$ has a unique Lévy-Khintchine representation

$$g(t) = \kappa t + \int_0^\infty (1 - \exp(-\lambda t)) \mu(d\lambda), \quad (11)$$

where $\kappa \geq 0$, and μ is a measure over $[0, \infty)$ such that $\int_0^\infty \min\{1, \lambda\} \mu(d\lambda) < \infty$. Comparing (9) and (11), we have $\kappa = \nu(\{0\})$ and $\mu = \tilde{\nu}$. The condition $\int_0^\infty \min\{1, \lambda\} \mu(d\lambda) < \infty$ is equivalent to Condition (2).

From (3) and (10), for $k = 1, 2, \dots$

$$\psi^{(k)}(t) = (-1)^{k+1} \frac{k!}{t^k} E(N_k(t)). \quad (12)$$

Analogous expression for (12) appears in Béguinot [2016] as an approximate formula under the multinomial model for fixed total number of observed individuals for the

species-sample-size curve with the derivative operator replaced by the difference operator. From (8), the log-likelihood function can be re-expressed as

$$\log(\mathcal{L}(\psi \mid \tilde{n}(t_0))) = -\psi(t_0) + \sum_{k=1}^{\infty} n_k(t_0) \log(|\psi^{(k)}(t_0)|). \quad (13)$$

Let us consider the power expansion of $\psi(t)$.

$$\begin{aligned} \psi(t) &= \int \frac{1 - \exp(-\lambda t_0)}{\lambda} \nu(d\lambda) - \int \frac{(\exp(\lambda(t_0 - t)) - 1) \exp(-\lambda t_0)}{\lambda} \nu(d\lambda) \\ &= E(N_+(t_0)) + \sum_{k=1}^{\infty} (-1)^{k+1} E(N_k(t_0)) \left(\frac{t}{t_0} - 1\right)^k. \end{aligned} \quad (14)$$

Equation (14) can be re-expressed as

$$\psi(t) = E(N_+(t_0)) \left(1 - \sum_{k=1}^{\infty} p_k(t_0) \left(1 - \frac{t}{t_0}\right)^k\right). \quad (15)$$

Equations (7), (11), and (15) establishes the one-to-one correspondence among the following three parametrizations of the mixed Poisson partition process: (i) the species intensity measure ν (or $\nu(\{0\})$ and $\tilde{\nu}$ as a whole), (ii) the ESAC $\psi(t)$ which is a Bernstein function passing through the origin, and (iii) the SAD $p(t_0)$ in the form of (7) together with $E(N_+(t_0))$ at any fixed t_0 .

Equation (14) implies that Good-Toulmin estimator [Good and Toulmin, 1956]

$$\hat{\psi}(t) = n_+(t_0) + \sum_{k=1}^{\infty} (-1)^{k+1} n_k(t_0) \left(\frac{t}{t_0} - 1\right)^k$$

is an unbiased estimator of $\psi(t)$ under the framework. This estimator works well in interpolation (i.e. $0 \leq t \leq t_0$), and performs satisfactorily in short-term extrapolation when $t_0 < t \leq 2t_0$. The curve $\hat{\psi}(t)$ for $0 \leq t \leq t_0$ is known as the rarefaction curve where a more intuitive expression is $\hat{\psi}(t) = \sum_{k=1}^{\infty} n_k(t_0)(1 - (1 - t/t_0)^k)$ when $0 \leq t \leq t_0$ because each species with frequency k at time t_0 has probability $(1 - (1 - t/t_0)^k)$ to be observed before time t (similar expression appears in Arrhenius [1921] where time is replaced by area).

We can deduce the following estimator for different order of derivative of $\psi(t)$ from the rarefaction curve.

$$\hat{\psi}^{(j)}(t) = \frac{1}{t_0^j} \sum_{k=j}^{\infty} \frac{\Gamma(k+1)n_k(t_0)}{\Gamma(k-j+1)} \left(1 - \frac{t}{t_0}\right)^{k-j}, \quad (j \geq 1), \quad (16)$$

where $\Gamma(x)$ is the gamma function.

Estimator in (16) is useful. For example, a concave downward curve when we plot $1/\hat{\psi}^{(1)}(t)$ for $t \in [0, t_0]$ is an indication that $E(D) = \infty$ because if there is a linear function $b + ct$ with positive b and c such that $b + ct \geq 1/\psi^{(1)}(t)$ for all $t \geq 0$. Then

$$E(D) = \int_0^\infty \psi^{(1)}(x)dx \geq \int_0^\infty (b + cx)^{-1}dx = \infty.$$

5 Derivative Ratio

A way to study a SAD is to consider the probability ratio, $p_j(t)/p_{j+1}(t)$ for $j = 1, 2, \dots$. It is equivalent to examine $-\psi^{(j)}(t)/\psi^{(j+1)}(t)$ ($= tp_j(t)/[(j+1)p_{j+1}(t)]$), which we call the j th derivative ratio. From (10) and the Cauchy-Schwarz inequality, for $j = 1, 2, \dots$ and $t \geq 0$, $\psi^{(j)}(t)\psi^{(j+2)}(t) \geq (\psi^{(j+1)}(t))^2$. It deduces that j th derivative ratio is always a nonnegative nondecreasing function of t . A sufficient condition for a function $\xi(t)$ on $[0, \infty)$ to be the first derivative ratio of an ESAC is that (i) $\xi(t)$ is a Bernstein function, and (ii) $\xi(0) > 0$ or $\xi^{(1)}(0) > 1$ (proof is given in Appendix C). We use $\xi(t)$ to denote the first derivative ratio.

The simplest nontrivial Bernstein function is the positive linear function on $[0, \infty)$. We call the family of ESACs with $\xi(t) = b + ct$, the linear first derivative ratio family, and denote it as LDR_1 . Clearly $b \geq 0$ and $c \geq 0$. If $b = 0$, c must be larger than 1 (see the condition (ii) in the above sufficient condition), otherwise $\psi(t)$ is infinite for finite t as seen from (17). Fixing $\psi^{(1)}(1) = a > 0$,

$$\psi(t) = \begin{cases} \frac{a(b+c)}{c-1} \left(\left(\frac{b+ct}{b+c} \right)^{1-1/c} - \left(\frac{b}{b+c} \right)^{1-1/c} \right) & (c \neq 0, 1), \\ ab \exp(1/b)(1 - \exp(-t/b)) & (c = 0), \\ a(b+1) \log(1 + (t/b)) & (c = 1). \end{cases} \quad (17)$$

Parameter a is a scale parameter. For $k = 1, 2, \dots$,

$$\psi^{(k)}(t) = \begin{cases} (-1)^{k+1} \frac{a(b+c)^{1-k} c^{k-1} t^k \Gamma(1/c+k-1)}{\Gamma(1/c)} \left(\frac{b+ct}{b+c} \right)^{1-1/c-k} & (c > 0), \\ (-1)^{k+1} ab^{1-k} \exp((1-t)/b) & (c = 0). \end{cases} \quad (18)$$

From (12) and (18), for $k = 1, 2, \dots$,

$$E(N_k(t)) = \begin{cases} \frac{a(b+c)^{1-k} c^{k-1} t^k \Gamma(1/c+k-1)}{k! \Gamma(1/c)} \left(\frac{b+ct}{b+c} \right)^{1-1/c-k} & (c > 0), \\ ab^{1-k} t^k \exp((1-t)/b)/k! & (c = 0). \end{cases} \quad (19)$$

It can be shown that $\nu(\{0\}) = 0$, and

$$\tilde{\nu}(d\lambda) = \begin{cases} \frac{a((b+c)/c)^{1/c}\lambda^{1/c-2}}{\Gamma(1/c)} \exp(-b\lambda/c)d\lambda & (c > 0), \\ ab \exp(1/b)\delta_{1/b}(d\lambda) & (c = 0), \end{cases} \quad (20)$$

where $\delta_{1/b}(A) = \mathbf{1}\{1/b \in A\}$ is the Dirac measure. The intensity function $\tilde{\nu}$ takes the form as a gamma distribution with extended shape parameter $1/c - 1$ for nonnegative c . Therefore, $p(t)$ is the Engen's extended negative binomial distribution [Engen, 1974] with support $\{1, 2, \dots\}$. Engen's extended negative binomial distribution also appears in the model studied by Zhou et al. [2017]. The Hill number of order q for LDR_1 is

$${}^qD_\nu = \begin{cases} ab \exp(1/b) & (c = 0) \\ a((b+c)/b)^{1/c}(b/c)(\Gamma(1/c+q-1)/\Gamma(1/c))^{1/(1-q)} & (c > 0, q > 1 - 1/c, q \neq 1) \\ a((b+c)/b)^{1/c}(b/c) \exp(-\Psi(1/c)) & (c > 0, q = 1) \\ \infty & (c > 0, q \leq 1 - 1/c). \end{cases} \quad (21)$$

where $\Psi(x) = d(\log(\Gamma(x)))/dx$ is the digamma function. $E(D)$ can be found either as ${}^0D_\nu$ or $\lim_{t \rightarrow \infty} \psi(t)$. If $\psi(t) \in \text{LDR}_1$, $E(D) = {}^0D_\nu = \infty$ if and only if $c \geq 1$. In this case, $E(N_k(t))$ keeps increasing as t increases for any fixed k . When $E(D) < \infty$, $E(N_k(t))$ is unimodal with respect to t .

From (19), it can be shown that for $j = 1, 2, \dots$,

$$\frac{p_j(t)p_{j+2}(t)}{p_{j+1}^2(t)} = \frac{(j+1)(jc+1)}{(j+2)((j-1)c+1)}. \quad (22)$$

When $0 \leq c < 1$, $E(N_0(t)) (= E(D) - \psi(t))$ is finite. Define $p_0(t) = E(N_0(t))/E(N_+(t))$ (it is not a probability and can be larger than 1). It can be proved that when $0 \leq c < 1$, (22) holds also when $j = 0$. Therefore, when $0 \leq c < 1$,

$$E(N_0(t)) = \frac{p_1(t)^2 E(N_+(t))}{2(1-c)p_2(t)} = \frac{E^2(N_1(t))}{2(1-c)E(N_2(t))}. \quad (23)$$

Equation (23) portrays a relation among rare species. Thus c in (23) can be interpreted as the c -parameter of the LDR_1 for the rare species instead of for all species. An estimate of c , say \tilde{c} can be found from solving (22) for c when $j = 1$ with all $p_j(t_0)$'s replaced by their relative frequency estimates.

$$\tilde{c} = 3n_1(t_0)n_3(t_0)/(2n_2^2(t_0)) - 1. \quad (24)$$

As theoretically $c \geq 0$, an improved estimate of c is $\hat{c}^* = \max(\tilde{c}, 0)$. We can then estimate $E(N_0(t_0))$ using (23) with all unknowns replaced by their estimates. As $E(D) = E(N_+(t_0)) + E(N_0(t_0))$, an estimate of $E(D)$ is

$$\hat{E}^*(D) = \begin{cases} n_+(t_0) + n_1^2(t_0)/[2(1 - \hat{c}^*)n_2(t_0)] & \text{if } \hat{c}^* < 1 \\ \infty & \text{if } \hat{c}^* \geq 1. \end{cases} \quad (25)$$

This estimator is applicable when the data for rare species follows LDR_1 and all abundant species are assumed having been seen in the study (thus their contribution to D has already been included in $n_+(t_0)$). If $\hat{c}^* = 0$ (from (20), $c = 0$ corresponds to the case when all species have the same rate), $\hat{E}^*(D)$ is the Chao1 estimator [Chao, 1984].

Family LDR_1 includes the following existing models. Most of them have simple form of $\psi^{(1)}(t)$ which facilitates easy graphical check.

- Case $c = 0$: Zero-truncated Poisson distribution for the SAD, negative exponential law for the ESAC.

When $c = 0$, $E(N_k(t)) = ab \exp(1/b)(t/b)^k \exp(-t/b)/k!$ is proportional to a zero-truncated Poisson distribution. It is the simplest SAD with all species having the same rate $1/b$. The ESAC is $\psi(t) = ab \exp(1/b)(1 - \exp(-t/b))$ which is the negative exponential law. A diagnostic graph specially designed for it is to plot $\log(\hat{\psi}^{(1)}(t))$ against $t \in [0, t_0]$ for $\hat{\psi}^{(1)}(t)$ defined in (16). If the model is correct, we should see a curve close to a straight line because $\log(\psi^{(1)}(t)) = 1/b + \log(a) - t/b$.

- Case $0 < c < 1$: Zero-truncated negative binomial distribution for the SAD.

When $0 < c < 1$, $\tilde{\nu}$ is proportional to a gamma probability measure, and $p(t)$ is the probability vector for the zero-truncated negative binomial distribution.

- Case $c = 1/2$: Geometric distribution for the SAD, hyperbola law for the ESAC.

A special value of c in $(0, 1)$ is $c = 1/2$. The $\tilde{\nu}$ is proportional to an exponential probability measure and $p(t)$ is a geometric probability vector. The ESAC is $\psi(t) = a(2b + 1)^2 t / (2b(t + 2b))$ which is the hyperbola law (also known as Michaelis-Menten equation and Monod model). A graph for this distribution is to plot $(\hat{\psi}^{(1)}(t))^{-1/2}$ as a function of $t \in [0, t_0]$. If geometric distribution fits the data, we should see an almost linear curve because $(\psi^{(1)}(t))^{-1/2} = (t + 2b)/(a^{1/2}(2b + 1))$.

- Case $c = 1$: Log-series distribution for the SAD, Kobayashi's logarithm law for the ESAC.

When $c = 1$, $E(N_k(t)) = a(b + 1)(t/(t + b))^k/k$ corresponding to the log-series distribution. The ESAC is $\psi(t) = a(b + 1)\log(1 + t/b)$ which was introduced in Kobayashi [1975] (see also Fisher et al. [1943] and May [1975]). A graph for the log-series distribution is to draw $1/\hat{\psi}^{(1)}(t)$ as a function of $t \in [0, t_0]$. If the model is good, the curve should be close to a straight line because $1/\psi^{(1)}(t) = (b + t)/(a(b + 1))$.

- Case $b = 0$ (it implies $c > 1$): Power law for the ESAC.

When $c > 1$ and $b = 0$, $\psi(t) = act^{1-1/c}/(c - 1)$ is the power law. For $k = 1, 2, \dots$,

$$p_k(t) = \frac{(c - 1)\Gamma(1/c + k - 1)}{k!c\Gamma(1/c)}, \quad (26)$$

which does not depend on t . Power law is the only ESAC having this property (proof is given in Appendix D). For example, at any time, the probability of singleton (species observed only once in the study) is $(c - 1)/c$. The probability vector in (26) also appears in Zhou et al. [2017]. From (17), when $c > 1$ and t is large, $\psi(t)$ in LDR_1 behaves like a power law. When c approaches infinity, $\psi(t)$ tends to at which corresponds to a population containing only zero-probability species. A graph to check the power law is to plot $\log(\hat{\psi}^{(1)}(t))$ against $\log(t)$. The curve should be approximately linear because $\log(\psi^{(1)}(t)) = \log(a) - c^{-1}\log(t)$. We call this plot, log(D)-log plot.

Currently a standard diagnostic plot for power law is the log-log plot which plots $\log(\hat{\psi}(t))$ against $\log(t)$. As $d\log(\psi(t))/d\log(t) = p_1(t)$, log-log plot detects whether $p_1(t)$ is a constant function. On the other hand, log(D)-log plot checks whether $p_2(t)/p_1(t)$ is a constant function because $d\log(\psi^{(1)}(t))/d\log(t) = -2p_2(t)/p_1(t)$. Log(D)-log plot is more sensitive to discrepancies with the power law because $p_1(t)$ changes very slowly with respect to t for many SADs. It is well-known in species-area relationship studies that the curve in log-log plot is approximately linear for various dissimilar SADs [Preston, 1960, 1962, May, 1975, Martin and Goldenfield, 2006].

We extend the linear first derivative ratio family to linear j th derivative ratio family, which we denote as LDR_j . A $\psi(t)$ belongs to LDR_j if $-\psi^{(j)}(t)/\psi^{(j+1)}(t)$ is a linear

function of t . We prove in Appendix E that $\text{LDR}_2 = \text{LDR}_3 = \dots$, and LDR_2 is simply a mixture of zero-probability species and LDR_1 (i.e. the $\tilde{\nu}$ of LDR_2 satisfies (20), but $\nu(\{0\})$ can be positive).

An advantage of LDR_1 is that it has a simple diagnostic plot: Draw $\hat{\xi}(t) = -\hat{\psi}^{(1)}(t)/\hat{\psi}^{(2)}(t)$ as a function of $t \in [0, t_0]$ for $\hat{\psi}^{(1)}(t)$ and $\hat{\psi}^{(2)}(t)$ defined in (16). If the curve in the plot is almost linear, LDR_1 is an appropriate model. We call the plot, D1/D2 plot. Similarly, to investigate how well LDR_2 fits a data, we can plot the function $-\hat{\psi}^{(2)}(t)/\hat{\psi}^{(3)}(t)$ for $t \in [0, t_0]$ where $\hat{\psi}^{(2)}(t)$ and $\hat{\psi}^{(3)}(t)$ are defined in (16). We call the plot, D2/D3 plot.

By the delta method, we can approximate $\text{Var}(\hat{\xi}(t))$ by

$$\widehat{\text{Var}}(\hat{\xi}(t)) = \frac{\widehat{\text{Var}}(\hat{\psi}^{(1)}(t))}{\hat{\psi}^{(2)2}(t)} + \frac{\hat{\psi}^{(1)2}(t)\widehat{\text{Var}}(\hat{\psi}^{(2)}(t))}{\hat{\psi}^{(2)4}(t)} - \frac{2\hat{\psi}^{(1)}(t)\widehat{\text{Cov}}(\hat{\psi}^{(1)}(t), \hat{\psi}^{(2)}(t))}{\hat{\psi}^{(2)3}(t)},$$

where

$$\widehat{\text{Var}}(\hat{\psi}^{(1)}(t)) = \frac{1}{t_0^2} \sum_{k=1}^{\infty} k^2 n_k(t_0) (1 - t/t_0)^{2k-2},$$

$$\widehat{\text{Var}}(\hat{\psi}^{(2)}(t)) = \frac{1}{t_0^4} \sum_{k=2}^{\infty} k^2 (k-1)^2 n_k(t_0) (1 - t/t_0)^{2k-4},$$

and

$$\widehat{\text{Cov}}(\hat{\psi}^{(1)}(t), \hat{\psi}^{(2)}(t)) = -\frac{1}{t_0^3} \sum_{k=2}^{\infty} k^2 (k-1) n_k(t_0) (1 - t/t_0)^{2k-3}.$$

We use $\hat{\xi}(t) \pm 1.96 \sqrt{\widehat{\text{Var}}(\hat{\xi}(t))}$ as an approximate 95% pointwise confidence band for the D1/D2 plot. Similar confidence band can be constructed for D2/D3 plot (see Appendix F).

D1/D2 plot is useful even when $\hat{\xi}(t)$ is not approximately linear. If we can judge from the $\hat{\xi}(t)$ in the D1/D2 plot that there are positive values b and t^* such that $\hat{\xi}(t) \geq b + t$ whenever $t \geq t^*$, then $E(D)$ is likely infinite. On the other hand, if $\hat{\xi}(t) \leq b + ct$ for a $0 \leq c < 1$, it is reasonable to believe that $E(D)$ is finite. The justification of above judgments is given in Appendix G.

6 An Extended Family of LDR_1

Abundant species are usually seen early in the survey and affect mainly the front part of $\xi(t)$, whereas the stochastic structure of rare species is reflected in the rear part

of $\xi(t)$. If a linear function does not fit the whole $\xi(t)$, the rear part of $\xi(t)$ can be approximately linear, which means that the rare species follow closely a LDR₁ model. A linear extrapolation of $\hat{\xi}(t)$ is the straight line passing through the end point $\hat{\xi}(t_0)$ with slope $\hat{\xi}^{(1)}(t_0) = \hat{\psi}^{(1)}(t_0)\hat{\psi}^{(3)}(t_0)/\psi^{(2)2}(t_0) - 1$. Using this slope to estimate the c of the LDR₁ model for the rare species, we find an estimator of c which is identical to \tilde{c} in (24). It gives another justification of the estimator $E^*(D)$.

A natural generalization of linear function is rational function in the form of the ratio between a quadratic function and a linear function. Consider the following partial fraction expansion of the inverse of the ratio $\xi(t) = 1/[c_1/(t + b_1) + c_2/(t + b_2)]$. For simplicity, we assume that b_2 and c_1 are positive parameters, and b_1 and c_2 are non-negative parameters such that $b_1 < b_2$. It ensures that $\xi(t)$ is a Bernstein function. We also require that if $b_1 = 0$ (thus $\xi(0) = 0$), then $c_1 < 1$ in order to ensure that $\psi(t)$ is finite for all finite t . We call this family of $\xi(t)$ the rational first derivative ratio family, and denote it as RDR₁. This form has the following advantages: (i) RDR₁ includes LDR₁ which can be observed by substituting $c_2 = 0$; (ii) as $t \rightarrow \infty$, the difference between $\xi(t)$ and the linear function $t/(c_1 + c_2) + (b_1c_1 + b_2c_2)/(c_1 + c_2)^2$ tends to zero, and hence $\xi(t)$ is asymptotically linear. It can be proved by mathematical induction that for $k \geq 1$,

$$k(k-1+c_1+c_2)\psi^{(k)}(t) + [c_1t + b_2c_1 + c_2t + b_1c_2 + k(2t + b_1 + b_2)]\psi^{(k+1)}(t) + (t+b_1)(t+b_2)\psi^{(k+2)}(t) = 0.$$

Choose a value for t_0 . Given $a = \psi^{(1)}(t_0)$ which is a scale parameter, and the values of the parameters b_1, b_2, c_1 and c_2 , we can find $\psi^{(2)}(t_0) = -\psi^{(1)}(t_0)/\xi(t_0)$ and then apply the above recurrence relation for $t = t_0$ to compute all necessary $\psi^{(k)}(t_0)$ in (13). As

$$\psi(t) = a(t_0 + b_1)^{c_1}(t_0 + b_2)^{c_2} \int_0^t (x + b_1)^{-c_1}(x + b_2)^{-c_2} dx,$$

the log-likelihood function can be computed numerically. Quantity $E(D) = \lim_{t \rightarrow \infty} \psi(t)$ is finite if and only if $c_1 + c_2 > 1$. It can be proved that $\nu(\{0\}) = 0$. Assume that c_1 and c_2 are both positive.

$$\frac{d\tilde{\nu}}{d\lambda} = \frac{a(t_0 + b_1)^{c_1}(t_0 + b_2)^{c_2} \exp(-b_1\lambda)\lambda^{c_1+c_2-2}}{\Gamma(c_1)\Gamma(c_2)} \int_0^1 y^{c_2-1}(1-y)^{c_1-1} \exp(-(b_2-b_1)\lambda y) dy.$$

Assume further that $b_1 > 0$, which implies that Λ is finite. When $q \geq 0$ and $q \neq 1$,

$${}^q D_\nu = a(t_0 + b_1)^{c_1} (t_0 + b_2)^{c_2} \left(\frac{b_1^{c_1 q} b_2^{c_2 q} \Gamma(c_1 + c_2 + q - 1)}{\Gamma(c_1) \Gamma(c_2)} \int_0^1 y^{c_2 - 1} (1 - y)^{c_1 - 1} ((b_2 - b_1)y + b_1)^{-c_1 - c_2 - q + 1} dy \right)^{1/(1-q)}.$$

When $q = 1$,

$${}^1 D_\nu = a \left(\frac{t_0 + b_1}{b_1} \right)^{c_1} \left(\frac{t_0 + b_2}{b_2} \right)^{c_2} \exp \left(- \frac{b_1^{c_1} b_2^{c_2}}{B(c_1, c_2)} \int_0^1 y^{c_2 - 1} (1 - y)^{c_1 - 1} \frac{\Psi(c_1 + c_2) - \log((b_2 - b_1)y + b_1)}{((b_2 - b_1)y + b_1)^{c_1 + c_2}} dy \right),$$

where $B(x, y)$ is the Beta function.

7 Examples

Three real FoF data are presented in Table 1. Nonparametric analysis of the data can be found in Böhning and Schön [2005], Lijoi, Mena, and Prünster [2007], Wang [2010], Chee and Wang [2016] and Chiu and Chao [2016]. Except for the second dataset, $\hat{E}^*(D) = \infty$. In this section, we fit the data using the parametric models in Sections 5 and 6. Without loss of generality, we set $t_0 = 1$. The significance level of the tests is fixed to 5%.

The first data is the swine feces data which appeared and was analyzed in Chiu and Chao [2016]. It is for the pooled contig spectra from seven non-medicated swine feces. The large $n_1(t_0)$ relative to other frequencies is viewed as a signal for sequencing errors. Chiu and Chao [2016] proposed a nonparametric estimate of the singleton count basing on the other counts, and the difference of this estimate and the observed singleton count is interpreted as outcome of missequencing. An implicit assumption of this approach is that sequencing errors inflate only the singleton count, and all other frequency counts are unaffected. It is equivalent to claim that there are sequencing errors which create solely zero-probability species.

To investigate whether zero-probability species really exist, we draw the D1/D2 and D2/D3 plots with 95% pointwise confidence bands in panels (a) and (b) respectively in Figure 2. The approximate linear curve in both plots indicates that both LDR_1 and LDR_2 are reasonable models. The heavy dashed lines in panels (a) and (b) are

Table 1: Three real FoF data (the values \hat{a} , \hat{b} and \hat{c} are MLE under LDR₁ model, and ${}^0\hat{D}_\nu$, ${}^1\hat{D}_\nu$ and ${}^2\hat{D}_\nu$ are respectively the MLE of ${}^0D_\nu$, ${}^1D_\nu$ and ${}^2D_\nu$ under the selected model)

(i) Swine feces data ($\hat{a} = 8027.6, \hat{b} = 2.878, \hat{c} = 3.963$ under LDR₁,
 ${}^0\hat{D}_\nu = \infty, {}^1\hat{D}_\nu = 477568, {}^2\hat{D}_\nu = 28745$ under LDR₁)

| | | | | | | | | | | | |
|------------|------|-----|-----|----|----|---|---|---|---|----|----|
| k | 1 | 2 | 3 | 4 | 5 | 6 | 7 | 8 | 9 | 10 | 11 |
| $n_k(t_0)$ | 8025 | 605 | 129 | 41 | 16 | 8 | 4 | 2 | 1 | 1 | 1 |

(ii) Accident data ($\hat{a} = 1320.3, \hat{b} = 1.817, \hat{c} = 1.115$ under LDR₁,
 ${}^0\hat{D}_\nu = \infty, {}^1\hat{D}_\nu = 7072, {}^2\hat{D}_\nu = 3685$ under LDR₁)

| | | | | | | | |
|------------|------|-----|----|----|---|---|---|
| k | 1 | 2 | 3 | 4 | 5 | 6 | 7 |
| $n_k(t_0)$ | 1317 | 239 | 42 | 14 | 4 | 4 | 1 |

(iii) Tomato flowers data ($\hat{a} = 1444.3, \hat{b} = 0.739, \hat{c} = 2.578$ under LDR₁,
 ${}^0\hat{D}_\nu = \infty, {}^1\hat{D}_\nu = 5941, {}^2\hat{D}_\nu = 1311$ under RDR₁)

| | | | | | | | | | | | | | | | | | |
|------------|------|-----|----|----|----|---|---|---|---|----|----|----|----|----|----|----|----|
| k | 1 | 2 | 3 | 4 | 5 | 6 | 7 | 8 | 9 | 10 | 11 | 12 | 13 | 14 | 16 | 23 | 27 |
| $n_k(t_0)$ | 1434 | 253 | 71 | 33 | 11 | 6 | 2 | 3 | 1 | 2 | 2 | 1 | 1 | 1 | 2 | 1 | 1 |

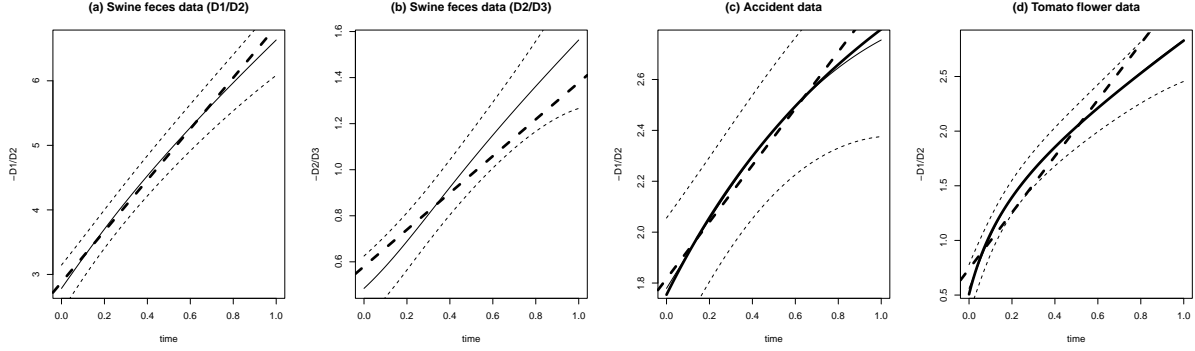


Figure 2: D1/D2 and D2/D3 plots for the data. The light solid curves are the D1/D2 or D2/D3 curve. The light dashed curves are the 95% pointwise confidence bands. The heavy dashed lines are the lines fitted by MLE under LDR_1 . The heavy solid curves in panels (c) and (d) are the MLE fitted curves under RDR_1 . The heavy and light solid curves are so close that it is hard to distinguish the twos in the plots except in the right end in panel (c).

the lines fitted by MLE under LDR_1 . The fitted line is close to the curve in D1/D2 plot, but is not so in the D2/D3 plot. As the dashed line lies inside the confidence bands in panel (b), the disagreement between the singleton count and other counts is not strong enough to reject that they come from the fitted LDR_1 . The Pearson's chi-square test statistic after grouping all cells with expected frequency less than 5 is 4.325 with 4 degrees of freedom. The estimated $E(N_1(t_0))$ under this LDR_1 is 8027.6 which is marginally larger than $n_1(t_0)$. As $\hat{E}(N_1(t_0)) > n_1(t_0)$, the MLE of $\nu(\{0\})$ under LDR_2 should be zero, and LDR_1 is our selected model. There is no significant evidence for the existence of zero-probability species.

The second data come from 9461 accident insurance policies issued by an insurance company. It was used in Böhning and Schön [2005], Wang [2010] and Chee and Wang [2016]. The species corresponds to the policies, and the frequency count to the number of claims during a particular year. The $\hat{\xi}(t)$ in the D1/D2 plot for the accident data in panel (c) is quite linear. The p-value for the Pearson chi-square test is 0.0979. The MLE of c is 1.1146, and an approximate 95% confidence interval for c is $[0.7499, 1.5485]$ which overlaps with $[0, 1)$. It means that $\hat{E}(D) = \infty$, but the hypothesis that $E(D)$ is finite is not rejected. The heavy solid curve in panel (c) is the fitted curve under RDR_1 .

The likelihood-ratio test shows that RDR_1 is not statistically better than LDR_1 . The MLE of $E(D)$ under RDR_1 is 6353. It is less than the true value $D = 9461$, and is comparable to the nonparametric estimates presented in Chee and Wang [2016] which ranges from 4016 to 7374. For this data, $\hat{c}^* = 0.4525$ and $\hat{E}^*(D) = 8249.2$ which is closer to the true value.

The last data come from a CDNA library of the expressed sequence tags of tomato flowers. It was studied in Böhning and Schön [2005] and Lijoi, Mena, and Prünster [2007]. The D1/D2 plot in panel (d) shows that LDR_1 model does not fit the data well. The curve looks like a Bernstein function. An RDR_1 model is fitted and the fitted curve is shown in the plot by a heavy solid curve. It almost coincides with the D1/D2 curve. The model fits the data well (Pearson's chi-square statistic after grouping all cells with expected frequency less than 5 is 1.470 with 2 degrees of freedom). It is significantly better than LDR_1 model. The MLE of b_1 , b_2 , c_1 and c_2 are 0.050, 1.451, 0.074 and 0.693 respectively. As $\hat{c}_1 + \hat{c}_2 = 0.767 < 1$, the estimated $E(D)$ is infinity.

8 ρ -appearance Design

Usually we collect all available information within the survey period. Under our framework, all useful information is in FoF. If labor saving is our concern, we may neglect some minor information, say halt recording a species as soon as its frequency reaches a fixed positive integer ρ in the study period $[0, t_0]$. In this case, the observation period for each species varies. The period is short for abundant species, and long for rare species. We call this design, the ρ -appearance design. This design places more emphasis on rare species than abundant species which is in line with the common understanding that information about the rare species is critical when our interest is in D . In bird survey, species can be identified by distant sightings or short bursts of song. Stop recording abundant species early helps the researcher concentrating more on the rare species. When $\rho = \infty$, we obtain $\tilde{n}(t_0)$. When $\rho = 1$, we record only the first appearance-time of each seen species. It is exactly the information available in the empirical SAC.

Suppose we call the recorded species with frequency less than ρ as rare species,

and all other recorded species as abundant species. For each seen species, say species i , we record (R_i, J_i) . For rare species, $(R_i, J_i) = (t_0, J_i)$ where J_i is the frequency of species i in the whole study period $[0, t_0]$. No information is lost for rare species. For abundant species, $(R_i, J_i) = (R_i, \rho)$ where R_i is the appearance time of the ρ th individual of species i . We call R_i , the ρ -appearance time of species i . We do not know the actual frequency of abundant species in $[0, t_0]$. The values $n_1(t_0), \dots, n_{\rho-1}(t_0)$ and $n_+(t_0)$ are still available. It is proved in Appendix H that the log-likelihood function given a realization of $\{(R_i, J_i)\}_i$, say $\{(r_i, j_i)\}_i$ is

$$\log(\mathcal{L}(\psi \mid \{r_i, j_i\}_i)) = -\psi(t_0) + \sum_{j=1}^{\rho-1} n_j(t_0) \log(|\psi^{(j)}(t_0)|) + \sum_{r_i < t_0} \log(|\psi^{(\rho)}(r_i)|). \quad (27)$$

An advantage of ρ -appearance design is that the log-likelihood function is simple even for complicated $\psi(t)$ because it depends only on the leading ρ derivatives of $\psi(t)$. A small simulation experiment in Appendix I shows that the loss in information of ρ -appearance design when compared to the standard design is marked when $\rho = 1$, and minor when $\rho = 4$.

By the displacement theorem of Poisson process [Kingman, 1993], the ρ -appearance times form a Poisson process with intensity function

$$f_\rho(r) = \int \frac{(\lambda r)^{\rho-1} e^{-\lambda r}}{(\rho-1)!} \nu(d\lambda) = \frac{r^{\rho-1}}{(\rho-1)!} (-1)^{\rho-1} \psi^{(\rho)}(r). \quad (28)$$

From (12), another expression for $f_\rho(r)$ is $f_\rho(r) = \rho E(N_\rho(r))/r$. Equation (28) gives another interpretation of $\psi^{(k)}(t)$. For example, $\psi^{(1)}(r)$ is the intensity function of the 1-appearance times, and $r|\psi^{(2)}(r)|$ is the intensity function of the 2-appearance times.

9 Inference on Empirical Species Accumulation Curve

Suppose we only observe the empirical SAC, $n_+(t)$ for $t \in [0, t_0]$, or equivalently, the 1-appearance times of all seen species (i.e., the case $\rho = 1$ in Section 8). Let $r_1, \dots, r_{n_+(t_0)}$ be the 1-appearance times observed in $[0, t_0]$. From (27), the log-likelihood function is

$$\log(\mathcal{L}(\psi \mid \{r_i\})) = \sum_{i=1}^{n_+(t_0)} \log(\psi^{(1)}(r_i)) - \psi(t_0).$$

If $\psi(t)$ has a free scale parameter, MLE of $\psi(t_0)$ is $n_+(t_0)$. The MLE of $\psi(t)$ for power law has a simple closed form $n_+(t_0)(t/t_0)^z$, where $z = \min\{n_+(t_0)/\sum_i \log(t_0/r_i), 1\}$.

Given a parametric form of $\psi(t)$, a traditional approach is to fit it to the empirical SAC by linear or non-linear least-squares method. Two differences between the MLE approach and the curve-fitting method are noteworthy. First, the MLE of $\psi(t_0)$ is equal to $n_+(t_0)$ whenever $\psi(t)$ has a free scale parameter, and it is not the case in the curve-fitting approach. Second, the MLE method fits the 1-appearance times to its density function $\psi^{(1)}(t)/\psi(t_0)$, while the curve-fitting method fits a distribution function to the empirical distribution function directly. The curve-fitting methods do not take the interdependence among the points in the empirical SAC into consideration. Since such interdependence is present in species-time curves and Type I species-area curves [Scheiner, 2003], the curve-fitting approach is theoretically flawed.

In certain situations, only the values of the empirical SAC at a finite set of points are available. For example, only the cumulative number of species observed after day 1, day 2, and so on are recorded. Suppose the observed $N_+(\ell_i)$ is $n_+(\ell_i)$ for $i = 1, \dots, m$ with $0 = \ell_0 < \ell_1 < \dots < \ell_m = t_0$. The log-likelihood function is

$$\log(\mathcal{L}(\psi \mid \{n_+(\ell_i)\}_{i=1,\dots,m})) = \sum_{i=1}^m (n_+(\ell_i) - n_+(\ell_{i-1})) \log(\psi(\ell_i) - \psi(\ell_{i-1})) - n_+(t_0) \log(\psi(t_0)).$$

In the simulation study in Appendix J, MLE has smaller root mean squared relative error in extrapolation when compared to the curve-fitting method.

The distribution function of the 1-appearance times in time interval $[0, t_0]$ is $\psi(t)/\psi(t_0)$. This fact holds generally and the only restriction on $\psi(t)$ is that $\psi(t)$ is nondecreasing and $\psi(0) = 0$. Apart from the ESACs under the mixed Poisson partition process, $\psi(t)$ can be sigmoid functions such as the cumulative Weibull function and the cumulative beta-P function. If we assume that the 1-appearance times are independent, we can perform maximum likelihood inference conditional on $n_+(t_0)$ when a parametric form of $\psi(t)$ is given. Full maximum likelihood calculation is possible when further assumption on the distribution of $N_+(t_0)$ is made. As the empirical SAC is proportional to the empirical distribution function of the 1-appearance times, statistical tools for empirical distribution function can be applied. For example we can apply the Dvoretzky-Kiefer-Wolfowitz inequality to construct confidence bands for the distribution function $\psi(t)/\psi(t_0)$.

10 Conclusion

The contributions of this paper are summarized as follows.

First, we introduce a general framework, called the mixed Poisson partition process which models the observed individuals for all species along the time axis. Parametric model can be defined by choosing a functional form for ν , $p(t)$, $\psi(t)$, $\psi^{(1)}(t)$ or $\xi(t)$. Each of them focuses on different aspects of the framework. Hill numbers under the framework are proposed.

Second, we introduce a family of ESAC, LDR_1 which accompanies a simple diagnostic plot, D1/D2 plot. We propose two extensions of LDR_1 : (i) LDR_2 which includes zero-probability species, and (ii) RDR_1 which approximates LDR_1 when t is large. We also suggest a handy estimator $\hat{E}^*(D)$ of $E(D)$ which is useful when the rare species behaves like LDR_1 .

Third, we introduce ρ -appearance design in which more effort is spent on rare species than abundant species.

Fourth, when only the empirical SAC is available, we show how MLE approach can be taken, and elucidate its advantages over the traditional curve-fitting method.

References

- Arrhenius, O. (1921). Species and area. *Journal of Ecology* **9**, 95–99.
- Béguinot, J. (2016). Extrapolation of the species accumulation curve associated to “chao” estimator of the number of unrecorded species: a mathematically consistent derivation. *Annual Research & Review in Biology* **11**, 1–19.
- Böhning, D. and Schön, D. (2005). Nonparametric maximum likelihood estimation of population size based on the counting distribution. *Journal of the Royal Statistical Society: Series C (Applied Statistics)* **54**, 721–737.
- Boneh, S., Boneh, A., and Caron, R. J. (1998). Estimating the prediction function and the number of unseen species in sampling with replacement. *Journal of the American Statistical Association* **93**, 372–379.

- Bulmer, M. G. (1974). On fitting the Poisson lognormal distribution to species-abundance data. *Biometrics* **30**, 101–110.
- Chao, A. (1984). Nonparametric estimation of the number of classes in a population. *Scandinavian Journal of Statistics* **11**, 265–270.
- Chee, C.-S. and Wang, Y. (2016). Nonparametric estimation of species richness using discrete k-monotone distributions. *Computational Statistics and Data Analysis* **93**, 107–118.
- Chiu, C.-H. and Chao, A. (2016). Estimating and comparing microbial diversity in the presence of sequencing errors. *PeerJ* **4**, 1634.
- Dengler, J. (2009). Which function describes the species–area relationship best? A review and empirical evaluation. *Journal of Biogeography* **36**, 728–744.
- Deolalikar, V. and Laffitte, H. (2016). Extensive large-scale study of error surfaces in sampling-based distinct value estimators for databases. *IEEE International Conference on Big Data* pp. 1579–1586.
- Dickie, I. A. (2010). Insidious effects of sequencing errors on perceived diversity in molecular surveys. *The New Phytologist* **188**, 916–918.
- Efron, B. and Thisted, R. (1976). Estimating the number of unseen species: How many words did Shakespeare know? *Biometrika* **63**, 435–447.
- Engen, S. (1974). On species frequency models. *Biometrika* **61**, 263–270.
- Fisher, R. A., Corbet, A. S., and Williams, C. B. (1943). The relation between the number of species and the number of individuals in a random sample of an animal population. *Journal of Animal Ecology* **12**, 42–58.
- Good, I. J. (1953). The population frequencies of species and the estimation of population parameters. *Biometrika* **40**, 237–264.
- Good, I. J. and Toulmin, G. (1956). The number of new species, and the increase in population coverage, when a sample is increased. *Biometrika* **43**, 45–63.

- Grøtan, V., Engen, S. and Grøtan, M. V. (2015). Package ‘poilog’. *Biometrics* **30**, 651–660.
- Haas, P. J., Naughton, J. F., Seshadri, S., and Stokes, L. (1995). Sampling-based estimation of the number of distinct values of a attribute. *VLDB* **95**, 311–322.
- Hill, M. O. (1973). Diversity and evenness: a unifying notation and its consequences. *Ecology* **54**, 427–432.
- Kingman, J. F. C. (1993). *Poisson Processes*. Oxford: Oxford University Press.
- Kobayashi, S. (1975). The species-area relation ii. a second model for continuous sampling. *Researches on Population Ecology* **16**, 265–280.
- Lijoi, A., Mena, R. H. and Prünster, I. (2007). Bayesian nonparametric estimation of the probability of discovering new species. *Biometrika* **94**, 769–786.
- Magurran, A. E. (2007). Species abundance distributions over time. *Ecology Letters* **10**, 347–354.
- Martin, H. G. and Goldenfield, N. (2006). On the origin and robustness of power-law species-area relationships in ecology. *PNAS* **103**, 10310–10315.
- Matthews, T. J. and Whittaker, R. J. (2014). Fitting and comparing competing models of the species abundance distribution: assessment and prospect. *Frontiers of Biogeography* **6**, 67–82.
- Matthews, T. J. and Whittaker, R. J. (2015). On the species abundance distribution in applied ecology and biodiversity management. *Journal of Applied Ecology* **52**, 443–454.
- May, R. M. (1975). Patterns of species abundance and diversity. In *Ecology and Evolution of Communities*, Eds. M. L. Cody & J. M. Diamond, pp.81–120. Cambridge: Belknap Press.
- Norris, J. L. and Pollock, K. H. (1998). Non-parametric MLE for Poisson species abundance models allowing for heterogeneity between species. *Environmental and Ecological Statistics* **5**, 391–402.

- Novotny, V. and Basset, Y. (2000). Rare species in communities of tropical insect herbivores: pondering the mystery of singletons. *Oikos* **89**, 564–572.
- Preston, F. W. (1960). Time and space and the variation of species. *Ecology* **41**, 612–627.
- Preston, F. W. (1962). The canonical distribution of commonness and rarity. *Ecology* **43**, 185–215.
- Raaijmakers, J. G. W. (1987). Statistical analysis of the Michaelis-Menten equation. *Biometrics* **43**, 793–803.
- Scheiner, S. M. (2003). Six types of species-area curves. *Global Ecology & Biogeography* **12**, 441–447.
- Tjørve, E. (2003). Shapes and functions of species-area curves: a review of possible models. *Journal of Biogeography* **30**, 827–835.
- Tjørve, E. (2009). Shapes and functions of species-area curves (ii): a review of new models and parameterizations. *Journal of Biogeography* **36**, 1435–1445.
- Trushkowsky, B., Kraska, T., Franklin, M. J., and Sarkar, P. (2012). Getting it all from the crowd. arXiv preprint arXiv:1202.2335.
- Wang, J.-P. (2010). Estimating species richness by a Poisson-compound gamma model. *Biometrika* **97**, 727–740.
- Williams, M. R., Lamont, B. B., and Henstridge, J. D. (2009). Species-area functions revisited. *Journal of Biogeography* **36**, 1994–2004.
- Zhou, M., Favaro, S., and Walker, S. G. (2017). Frequency of frequencies distributions and size-dependent exchangeable random partitions. *Journal of the American Statistical Association* **112**, 1623–1635.

Appendix A. Equivalent definition of the mixed Poisson partition process

In the definition of the mixed Poisson partition process in the paper, the individuals of the zero-probability species and the individuals of the positive-rate species are generated separately. Here we present an alternative definition where all individuals are generated in an unified manner.

Definition: (Equivalent definition of mixed Poisson partition process) A mixed Poisson partition process G is characterized by a species intensity measure ν , which is a measure over $\mathbb{R}_{\geq 0}$ satisfying $\int_0^\infty \min\{1, \lambda^{-1}\} \nu(d\lambda) < \infty$. Define $\dot{\nu}$ to be a measure over $\mathbb{R}_{\geq 0}^2$ by

$$\dot{\nu}(A) = \int \int_0^\infty \mathbf{1}\{(\lambda, t) \in A\} e^{-\lambda t} dt \cdot \nu(d\lambda)$$

for any measurable set $A \subseteq \mathbb{R}_{\geq 0}^2$ where $\mathbf{1}\{\cdot\}$ is the indicator function. Generate $(\lambda_1, t_1), (\lambda_2, t_2), \dots$ (a finite or countably infinite sequence) according to a Poisson process with intensity measure $\dot{\nu}$. For each simulated (λ_i, t_i) , we generate a realization η_i (independently across i) of a Poisson process with rate λ_i , conditioned on the event that the first point is at time t_i . (That is, it contains the point t_i together with a Poisson process starting at time t_i . If $\lambda_i = 0$, then η_i contains only one point t_i .) Finally, we take $G = \{\eta_1, \eta_2, \dots\}$.

This definition models the species that will eventually be observed in a study. The first appearance time for each of such species (i.e. the first point of each η_i) is explicitly included in the definition of $\dot{\nu}$.

Appendix B. Proof of the equivalence between Condition (2) and the finiteness of ESAC

Condition (2) is equivalent to $E(N_+(t)) < \infty$ for $t \geq 0$ because under Condition (2),

$$\int \frac{1 - \exp(-\lambda t)}{\lambda} \nu(d\lambda) \leq \int \min\{t, \lambda^{-1}\} \nu(d\lambda) \leq \max\{t, 1\} \int \min\{1, \lambda^{-1}\} \nu(d\lambda) < \infty$$

for $t \geq 0$, and if $E(N_+(1)) < \infty$, then

$$\int \min\{1, \lambda^{-1}\} \nu(d\lambda) \leq \frac{1}{1 - \exp(-1)} \int \frac{1 - \exp(-\lambda)}{\lambda} \nu(d\lambda) = \frac{E(N_+(1))}{1 - \exp(-1)} < \infty.$$

Appendix C. Proof of the sufficient condition of $\xi(t)$ in Section 5

Theorem: If $\xi(t)$ is a Bernstein function such that either $\xi(0) > 0$ or $\xi^{(1)}(0) > 1$, then there is an ESAC, $\psi(t)$ such that $\xi(t) = -\psi^{(1)}(t)/\psi^{(2)}(t)$.

Proof. We have $\xi(t) \geq 0$ for $t \in [0, \infty)$ and $\xi^{(1)}(0) > 1$ if $\xi(0) = 0$. Therefore, there exist $\epsilon > 0$ and $\delta > 0$ such that for all $0 < t < \delta$, we have $\xi(t) > (1 + \epsilon)t$. Let $g(t) = \delta \int_0^t \exp(\int_y^\delta (1/\xi(x))dx)dy$.

(i) Prove that $g(t)$ is finite when $t \geq 0$, and $g(0) = 0$.

When $0 < t \leq \delta$,

$$g(t) \leq \delta \int_0^\delta \exp\left(\int_y^\delta \frac{1}{(1+\epsilon)x} dx\right) dy = \delta \int_0^\delta \left(\frac{\delta}{y}\right)^{1/(1+\epsilon)} dy = \delta^2 \frac{1+\epsilon}{\epsilon} < \infty.$$

When $t > \delta$,

$$\begin{aligned} g(t) &= \delta \int_0^\delta \exp\left(\int_y^\delta (1/\xi(x))dx\right) dy + \delta \int_\delta^t \exp\left(\int_y^\delta (1/\xi(x))dx\right) dy \\ &\leq \delta^2(1+\epsilon)/\epsilon + \delta \int_\delta^t \exp\left(-\int_\delta^y (1/\xi(x))dx\right) dy \\ &\leq \delta^2(1+\epsilon)/\epsilon + \delta \int_\delta^t 1 dy \\ &= \delta^2(1+\epsilon)/\epsilon + \delta(t-\delta) < \infty. \end{aligned}$$

Therefore, $g(t)$ is finite for any $t > 0$. Obviously $g(0) = 0$.

(ii) Prove that $-g^{(1)}(t)/g^{(2)}(t) = \xi(t)$ and $g(t)$ is a Bernstein function.

We have $g^{(1)}(t) = \delta \exp(\int_t^\delta (1/\xi(x))dx)$, and $g^{(2)}(t) = -\delta \exp(\int_t^\delta (1/\xi(x))dx)(1/\xi(t))$. Thus $-g^{(1)}(t)/g^{(2)}(t) = \xi(t)$. Clearly $g(t)$ is positive and non-decreasing. As $g^{(2)}(t)\xi(t) = -g^{(1)}(t)$,

$$\sum_{i=0}^{k-2} \binom{k-2}{i} g^{(k-i)}(t)\xi^{(i)}(t) = -g^{(k-1)}(t) \quad (k \geq 2).$$

We prove by induction that $(-1)^{k-1}g^{(k)}(t) \geq 0$ for $k \geq 1$. Clearly it holds when $k = 1$.

Suppose it holds when $k \leq d$ for $d \geq 1$.

$$\sum_{i=0}^{d+1-2} \binom{d+1-2}{i} g^{(d+1-i)}(t)\xi^{(i)}(t) = -g^{(d)}(t).$$

Note that $\binom{d+1-2}{i} \geq 0$. For $i \geq 1$, $\text{sign}(g^{(d+1-i)}(t)\xi^{(i)}(t)) = \text{sign}((-1)^{d-i}(-1)^{i+1}) = (-1)^{d+1}$. Furthermore, $\text{sign}(-g^{(d)}(t)) = (-1)^d$. Thus $\text{sign}(g^{(d+1)}(t)\xi(t)) = (-1)^d$. It means that $\text{sign}(g^{(d+1)}(t)) = (-1)^d$ completing the proof by induction. Q.E.D.

Appendix D. Proof of the fact that power law is the only law with time-invariant species abundance distribution

Suppose $p(t) = p = (p_1, p_2, \dots)$ is a SAD which does not depend on t . For $k = 1, 2, \dots$,

$$p_k \psi(t) = E(N_k(t)) = \int \frac{\exp(-\lambda t) \lambda^{k-1} t^k}{k!} \nu(d\lambda).$$

Therefore, for any y ,

$$\left(\sum_{k=1}^{\infty} p_k (1-y)^k \right) \psi(t) = \int \frac{\exp(-\lambda t)}{\lambda} \sum_{k=1}^{\infty} \frac{((1-y)\lambda t)^k}{k!} \nu(d\lambda) = \psi(t) - \psi(yt).$$

It follows that

$$\psi(yt) = \psi(t) \left(1 - \sum_{k=1}^{\infty} p_k (1-y)^k \right).$$

Take logarithm on both sides, take derivative with respect to t , and then set $t = 1$. We have

$$\frac{d \log(\psi(y))}{dy} = \frac{\psi^{(1)}(1)}{\psi(1)y}.$$

The solution of the above differential equation is $\psi(y) = \psi(1)y^{\psi^{(1)}(1)/\psi(1)}$ which is the power law. Hence the power law is the only law with $p(t)$ independent on t .

Appendix E. Proof of $\text{LDR}_1 \subsetneq \text{LDR}_2 = \text{LDR}_3 = \dots$

For any positive integer j , condition $-\psi^{(j)}(t) = (b+ct)\psi^{(j+1)}(t)$ implies

$$-\psi^{(j+1)}(t) = c\psi^{(j+1)}(t) + (b+ct)\psi^{(j+2)}(t). \quad (29)$$

Therefore, $\text{LDR}_j \subseteq \text{LDR}_{j+1}$ for $j \geq 1$. Let $\phi(t) = \alpha t + \psi(t)$ where $\alpha > 0$ and $\psi(t) \in \text{LDR}_1$. Then $-\phi^{(2)}(t)/\phi^{(3)}(t) = -\psi^{(2)}(t)/\psi^{(3)}(t)$ which is a linear function of t because $\psi(t) \in \text{LDR}_1 \subseteq \text{LDR}_2$. Clearly $\phi(t) \in \text{LDR}_2$ but not in LDR_1 . Therefore, $\text{LDR}_1 \neq \text{LDR}_2$. It can be shown that every element in LDR_2 has the form $\alpha t + \psi(t)$ for a $\psi(t) \in \text{LDR}_1$. It means that LDR_2 is a mixture of zero-probability species and LDR_1 .

Consider $\psi(t) \in \text{LDR}_j$ for $j \geq 3$. Let $-\psi^{(j)}(t)/\psi^{(j+1)}(t) = b+ct$ (i.e. $d \log(\psi^{(j)}(t))/dt = -1/(b+ct)$). As j th derivative ratio is always a nonnegative nondecreasing function of t , both b and c are nonnegative. For simplicity, we only consider the case when $c > 0$

and $c \neq 1$ (cases when $c = 0$ and $c = 1$ can be studied through letting $c \rightarrow 0$ and $c \rightarrow 1$ respectively). Then

$$\psi^{(j)}(t) = \psi^{(j)}(1)[(b + ct)/(b + c)]^{-1/c}, \quad (30)$$

$$\psi^{(j-1)}(t) = \left[\psi^{(j-1)}(1) - \psi^{(j)}(1) \left(\frac{b+c}{c-1} \right) \right] + \psi^{(j)}(1) \left(\frac{b+c}{c-1} \right) \left(\frac{b+ct}{b+c} \right)^{1-1/c}, \quad (31)$$

and

$$\begin{aligned} \psi^{(j-2)}(t) &= \psi^{(j-2)}(1) + \left[\psi^{(j-1)}(1) - \psi^{(j)}(1) \left(\frac{b+c}{c-1} \right) \right] (t-1) \\ &\quad + \frac{(b+c)^2 \psi^{(j)}(1)}{(c-1)(2c-1)} \left[\left(\frac{b+ct}{b+c} \right)^{2-1/c} - 1 \right]. \end{aligned} \quad (32)$$

If $c > 1$ and $\psi^{(j)}(1) \neq 0$, from (31), $\text{sign}(\psi^{(j-1)}(t)) = \text{sign}(\psi^{(j)}(1)) \neq 0$ when t is large. It is impossible because they should have different sign. If $c > 1$ and $\psi^{(j)}(1) = 0$, from (30), $\psi^{(j)}(t)$ is a zero function. It is impossible because $-\psi^{(j)}(t)/\psi^{(j+1)}(t)$ is undefined. If $0 < c < 1$, from (31) and (32), $\text{sign}(\psi^{(j-1)}(t)) = \text{sign}(\psi^{(j-1)}(1) + \psi^{(j)}(1)[(b+c)/(1-c)]) = \text{sign}(\psi^{(j-2)}(t))$ when t is large. It is possible only when $\text{sign}(\psi^{(j-1)}(t)) = 0$. It implies that $\psi^{(j-1)}(1) + \psi^{(j)}(1)[(b+c)/(1-c)] = 0$. From (30) and (31), $-\psi^{(j-1)}(t)/\psi^{(j)}(t) = (b+ct)/(1-c)$ and $\psi(t) \in \text{LDR}_{j-1}$. It follows that $\text{LDR}_j = \text{LDR}_{j-1}$ for all $j \geq 3$.

Appendix F. Pointwise Confidence Band for D2/D3 plot

Similar to the confidence band for D1/D2 plot, an approximate 95% pointwise confidence band for D2/D3 plot is $-\hat{\psi}^{(2)}(t)/\hat{\psi}^{(3)}(t) \pm 1.96\sqrt{\widehat{\text{Var}}(-\hat{\psi}^{(2)}(t)/\hat{\psi}^{(3)}(t))}$, where

$$\begin{aligned} &\widehat{\text{Var}} \left(-\frac{\hat{\psi}^{(2)}(t)}{\hat{\psi}^{(3)}(t)} \right) \\ &= \frac{1}{\hat{\psi}^{(3)2}(t)} \widehat{\text{Var}}(\hat{\psi}^{(2)}(t)) + \frac{\hat{\psi}^{(2)2}(t)}{\hat{\psi}^{(3)4}(t)} \widehat{\text{Var}}(\hat{\psi}^{(3)}(t)) - \frac{2\hat{\psi}^{(2)}(t)}{\hat{\psi}^{(3)3}(t)} \widehat{\text{Cov}}(\hat{\psi}^{(2)}(t), \hat{\psi}^{(3)}(t)), \end{aligned}$$

with

$$\begin{aligned} \widehat{\text{Var}}(\hat{\psi}^{(2)}(t)) &= \frac{1}{t_0^4} \sum_{k=2}^{\infty} k^2(k-1)^2 n_k(t_0) \left(1 - \frac{t}{t_0} \right)^{2k-4}, \\ \widehat{\text{Var}}(\hat{\psi}^{(3)}(t)) &= \frac{1}{t_0^6} \sum_{k=3}^{\infty} k^2(k-1)^2(k-2)^2 n_k(t_0) \left(1 - \frac{t}{t_0} \right)^{2k-6}, \end{aligned}$$

and

$$\widehat{\text{Cov}}(\hat{\psi}^{(2)}(t), \hat{\psi}^{(3)}(t)) = -\frac{1}{t_0^5} \sum_{k=3}^{\infty} k^2(k-1)^2(k-2) n_k(t_0) \left(1 - \frac{t}{t_0} \right)^{2k-5}.$$

Appendix G. Use of D1/D2 plot in the detection of the finiteness of $E(D)$

Let $\xi_1(t)$ and $\xi_2(t)$ be the first derivative ratio of two ESACs, $\psi_1(t)$ and $\psi_2(t)$ respectively. Suppose $\xi_1(t) \geq \xi_2(t)$ for all $t \geq t^* > 0$. It means that

$$\frac{d(\log(\psi_1^{(1)}(t)/\psi_2^{(1)}(t)))}{dt} \geq 0$$

when $t \geq t^* > 0$. The function $\psi_1^{(1)}(t)/\psi_2^{(1)}(t)$ is a nondecreasing function on $[t^*, \infty)$.

For all $t > t^*$,

$$\begin{aligned} \psi_1(t) &= \psi_1(t^*) + \int_{t^*}^t \psi_1^{(1)}(x) dx \geq \psi_1(t^*) + \frac{\psi_1^{(1)}(t^*)}{\psi_2^{(1)}(t^*)} \int_{t^*}^t \psi_2^{(1)}(x) dx \\ &= \psi_1(t^*) + \frac{\psi_1^{(1)}(t^*)}{\psi_2^{(1)}(t^*)} (\psi_2(t) - \psi_2(t^*)). \end{aligned} \quad (33)$$

As $t^* > 0$, all values in the above expression are finite.

Suppose $\xi_1(t) \geq b + t$ for a positive constant b when $t \geq t^* > 0$. Since $b + t$ is $\xi_2(t)$ for a log-series distribution, and $\lim_{t \rightarrow \infty} \psi_2(t) = \infty$, from (33), $\lim_{t \rightarrow \infty} \psi_1(t) = \infty$ (i.e. $E(D) = \infty$).

Similarly suppose $\xi_2(t) \leq b + ct$ for a $0 \leq c < 1$. As the inequality always holds when we increase b , we can without loss of generality, assume $b > 0$. Thus $b + ct$ is $\xi_1(t)$ of a LDR_1 whose $\lim_{t \rightarrow \infty} \psi_1(t) < \infty$. From (33), $\lim_{t \rightarrow \infty} \psi_2(t) < \infty$.

Appendix H. Proof of the log-likelihood function for ρ -appearance design

For a species with rate λ , the probability function of J is

$$P(J = j \mid \lambda) = \begin{cases} \frac{(\lambda t_0)^j e^{-\lambda t_0}}{j!} & (j < \rho) \\ \sum_{k=\rho}^{\infty} \frac{(\lambda t_0)^k e^{-\lambda t_0}}{k!} & (j = \rho). \end{cases} \quad (34)$$

Since the time of the ρ th individual follows Erlang(ρ, λ) distribution,

$$P(R \in [r, r + dr), J = \rho \mid \lambda) = \frac{\lambda^\rho r^{\rho-1} e^{-\lambda r}}{(\rho - 1)!} dr. \quad (35)$$

By (34) and (35), the joint probability density function of the observations $\{(R_i, J_i)\}_{i \leq n_+(t_0)}$ given ν is proportional to

$$e^{-\psi(t_0)} \left(\prod_{i: j_i < \rho} \int \frac{\lambda^{j_i-1} t_0^{j_i} e^{-\lambda t_0}}{j_i!} \nu(d\lambda) \right) \left(\prod_{i: j_i = \rho} \int \frac{\lambda^{\rho-1} r_i^{\rho-1} e^{-\lambda r_i}}{(\rho - 1)!} \nu(d\lambda) \right).$$

Therefore, the log-likelihood function is

$$\log(\mathcal{L}(\psi \mid \{r_i, j_i\}_i)) = -\psi(t_0) + \sum_{j=1}^{\rho-1} n_j(t_0) \log(|\psi^{(j)}(t_0)|) + \sum_{r_i < t_0} \log(|\psi^{(\rho)}(r_i)|).$$

Appendix I. Simulation experiment on the loss of information of the ρ -appearance design

Consider the bird abundance data for the Wisconsin route of the North American Breeding Bird Survey for 1995. The data was studied in Norris and Pollock [1998] where a mixture of five Poisson models was fitted. The data, $(n_1(t_0), \dots, n_{54}(t_0))$ is (11,12,10,6,2,5,1,3,2,4,0,1,1,1,2,1,0,2,0,0,0,0,0,0,1,0,0,0,1,1,0,1,0,0,0,0,0,1,0,0,0, 0, 1, 0, 0,0,0,0,0,0,1,1). Totally 645 birds from 72 species are recorded. Let us consider $\nu(d\lambda) = \gamma \lambda f(\lambda \mid \mu, \sigma) d\lambda$ where $f(\lambda \mid \mu, \sigma)$ is the density function of Lognormal(μ, σ^2) distribution. The parameter γ is the expected total number of species. From Section 3, the maximum likelihood estimate of μ and σ is identical to the conditional maximum likelihood estimate of the corresponding Poisson-lognormal model [Bulmer, 1974]. The fitted lognormal mixing distribution is Lognormal($\hat{\mu}, \hat{\sigma}^2$) distribution with $\hat{\mu} = 1.23$ and $\hat{\sigma} = 1.30$. Let $\omega_i(\mu, \sigma) = P(Y = i)$ where Y is a Poisson-lognormal random variable with parameters μ and σ . We use the function “dpoilog” in R-package “poilog” [Grøtan, Engen, and Grøtan, 2015] to compute this probability. The estimated γ is $\hat{\gamma} = n_+(t_0)/(1 - \omega_0(\hat{\mu}, \hat{\sigma}^2)) = 85.2$.

Without loss of generality, set $t_0 = 1$. We use this data to investigate the information loss of the ρ -appearance design. The ρ -appearance data are simulated from the data using the following procedure:

Simulation procedure: Suppose species i has observed frequency m_i in time $[0, 1]$. If $m_i < \rho$, our data for this species is m_i , the frequency of it in time $[0, 1]$. If $m_i \geq \rho$, we simulate the ρ -appearance time of the species, r_i from Beta($\rho, m_i + 1 - \rho$) distribution, which is the distribution of the ρ order statistic of m_i samples from the $U(0, 1)$ distribution.

It can be shown that $E(N_k(t)) = \gamma\omega_k(\mu + \log(t), \sigma)$. The log-likelihood function is

$$\begin{aligned} & \log(\mathcal{L}(\gamma, \mu, \sigma \mid \{r_i, j_i\}_i)) \\ = & -\gamma(1 - \omega_0(\mu, \sigma)) + \sum_{k=1}^{\rho-1} n_k(1) \log(\gamma\omega_k(\mu, \sigma)) + \sum_{r_i < 1} \log(\gamma\omega_\rho(\mu + \log(r_i), \sigma)). \end{aligned}$$

The maximum likelihood estimate for $E(N_+(1)) = \gamma(1 - \omega_0(\mu, \sigma))$ is $n_+(1)$. The function that we need to maximize to find $\hat{\mu}$ and $\hat{\sigma}$ is

$$h(\mu, \sigma) = -n_+(1) \log(1 - \omega_0(\mu, \sigma)) + \sum_{k=1}^{\rho-1} n_k(1) \log(\omega_k(\mu, \sigma)) + \sum_{r_i < 1} \log(\omega_\rho(\mu + \log(r_i), \sigma)).$$

The maximum likelihood estimate of γ is $\hat{\gamma} = n_+(1)/(1 - \omega_0(\hat{\mu}, \hat{\sigma}))$. We consider $\rho = 1, 2, \dots, 6$. For each ρ -value, we simulate 100 independent sets of ρ -appearance data. For each simulated data, μ , σ and γ are estimated. The sample mean and sample standard deviation of the estimates are presented in Table A. Graphical display is given in Figure 3.

The mean of the estimate is close to that basing on $\tilde{n}(t_0)$. The standard deviation of the estimator decreases as ρ increases. From the simulation results, the standard deviation of the estimators when $\rho = 1$ is considerably worse than those when $\rho = 2$. Value $\rho = 4$ performs well for this data. The total number of species with frequency less than 4 is 33, around 46% of the seen species. Under 4-appearance design, we only need to record 221 individuals, around 34% of all seen individuals.

Appendix J. Simulation comparison of MLE method and curve fitting method in extrapolation when finite number of points in the empirical SAC are available

We consider three distributions: power law, log-series distribution and geometric distribution. The curve-fitting methods of the distributions are described below:

- (a) Power law: $\psi(t) = \tau t^{1-1/c}$. For curve fitting, we regress $\log(\psi(t))$ on $\log(t)$.
- (b) Log-series distribution: $\psi(t) = \tau \log(1 + t/b) / \log(1 + 1/b)$. For curve fitting, we regress $\psi(t)$ on $\log(t)$. It is the standard approximation method which assumes that $1 + t/b \approx t/b$.

Table A. Mean and standard deviation of MLE for North American breeding bird

| survey data (1995) | | | | | | | |
|------------------------|------|------|------|------|------|------|----------|
| ρ | 1 | 2 | 3 | 4 | 5 | 6 | ∞ |
| mean of $\hat{\mu}$ | 1.10 | 1.28 | 1.23 | 1.21 | 1.21 | 1.22 | 1.23 |
| sd of $\hat{\mu}$ | 0.56 | 0.09 | 0.07 | 0.04 | 0.04 | 0.03 | 0* |
| mean of $\hat{\sigma}$ | 1.39 | 1.24 | 1.29 | 1.29 | 1.31 | 1.30 | 1.30 |
| sd of $\hat{\sigma}$ | 0.48 | 0.15 | 0.13 | 0.08 | 0.09 | 0.07 | 0* |
| mean of $\hat{\gamma}$ | 90.4 | 83.8 | 85.0 | 85.5 | 85.7 | 85.3 | 85.2 |
| sd of $\hat{\gamma}$ | 18.7 | 2.52 | 2.32 | 1.38 | 1.56 | 1.29 | 0* |

* When $\rho = \infty$, we always observe the full data, and the sample standard deviation (sd) of the estimator across simulation is zero.

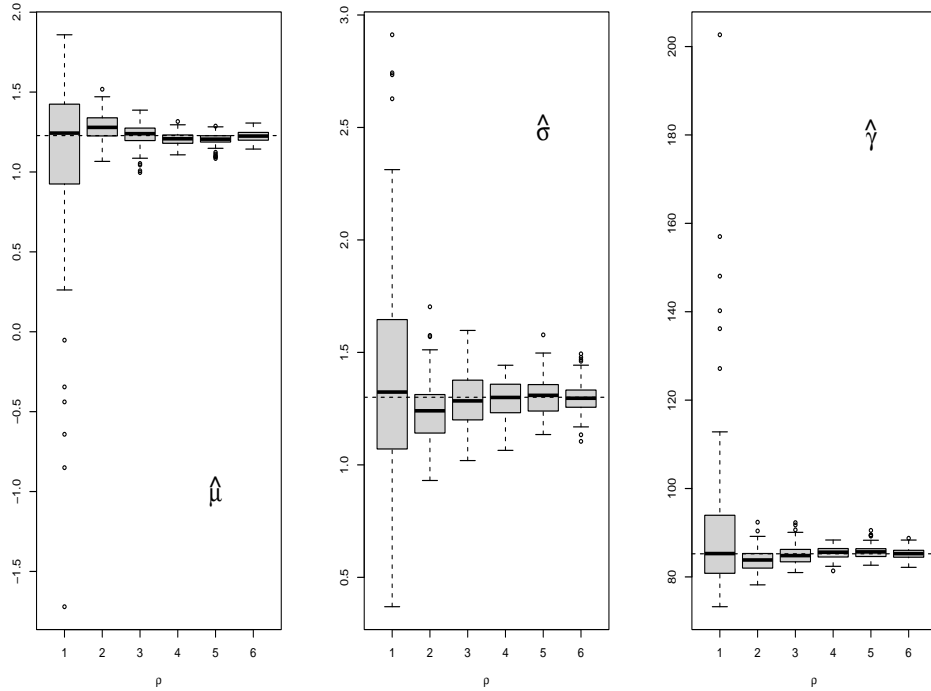


Figure 3: Box-and-whisker plots for estimators across different values of ρ in the simulation. The horizontal dashed line in each plot shows the estimate when the full Wisconsin route of the North American breeding bird survey data for 1995 is used. The variability of the estimate delineates the additional noise due to the ρ -appearance design.

(c) Geometric distribution (hyperbola law): $\psi(t) = \tau(1 + 2b)t/(t + 2b)$. There are various curve fitting methods for hyperbola law (see for example [Raaijmakers, 1987]). In this simulation, we use the simplest one, which regresses $1/\psi(t)$ on $1/t$.

With loss of generality, we set $t_0 = 1$. The parameter $\tau = \psi(1)$ is the expected number of recorded species at time $t_0 = 1$. In the experiment, τ can take value 200 and 1000. The distribution parameter can take 6 values. For power law, the value of c can be 1.25, 1.5, 2, 3, 4 and 5. For log-series distribution, the value of b can be 0.01, 0.02, 0.03, 0.05, 0.1, and 0.2. For geometric distribution, the value of b can be 0.05, 0.1, 0.2, 0.4, 0.6 and 0.8. Our data is $\{n_+(0.1), n_+(0.2), \dots, n_+(1)\}$. For each combination of parameters, we simulate 5000 data. The MLE estimate and curve-fitting estimate of $\psi(2)$ and $\psi(4)$ are found for each simulated data. We evaluate the performance of an estimator by the root mean squared relative error (RMSRE) (for estimator $\hat{\theta}$ for θ , $\text{RMSRE} = \sqrt{\sum_{i=1}^n ((\hat{\theta}_i - \theta)/\theta)^2/n}$). The results of the simulation are presented in Tables B, C and D. The RMSRE for MLE is smaller than that for the curve fitting method in this simulation study.

Table B. Simulation results for Power law

| Extrapolate to $t = 2$, $\psi(1) = 200$ | | | | | | |
|---|-------|-------|-------|-------|-------|-------|
| c | 1.25 | 1.5 | 2 | 3 | 4 | 5 |
| RMSRE(Curve-fitting) | 0.075 | 0.078 | 0.083 | 0.091 | 0.096 | 0.100 |
| RMSRE(MLE) | 0.073 | 0.074 | 0.077 | 0.080 | 0.082 | 0.083 |
| Extrapolate to $t = 2$, $\psi(1) = 1000$ | | | | | | |
| c | 1.25 | 1.5 | 2 | 3 | 4 | 5 |
| RMSRE(Curve-fitting) | 0.034 | 0.035 | 0.037 | 0.040 | 0.042 | 0.044 |
| RMSRE(MLE) | 0.033 | 0.034 | 0.035 | 0.036 | 0.037 | 0.037 |
| Extrapolate to $t = 4$, $\psi(1) = 200$ | | | | | | |
| c | 1.25 | 1.5 | 2 | 3 | 4 | 5 |
| RMSRE(Curve-fitting) | 0.081 | 0.089 | 0.103 | 0.120 | 0.132 | 0.140 |
| RMSRE(MLE) | 0.078 | 0.084 | 0.093 | 0.103 | 0.109 | 0.112 |
| Extrapolate to $t = 4$, $\psi(1) = 1000$ | | | | | | |
| c | 1.25 | 1.5 | 2 | 3 | 4 | 5 |
| RMSRE(Curve-fitting) | 0.036 | 0.040 | 0.045 | 0.052 | 0.057 | 0.060 |
| RMSRE(MLE) | 0.035 | 0.038 | 0.042 | 0.046 | 0.049 | 0.050 |

Table C. Simulation results for log-series distribution

| Extrapolate to $t = 2, \psi(1) = 200$ | | | | | | |
|--|-------|-------|-------|-------|-------|-------|
| b | 0.01 | 0.02 | 0.03 | 0.05 | 0.1 | 0.2 |
| RMSRE(Curve-fitting) | 0.073 | 0.073 | 0.073 | 0.077 | 0.090 | 0.122 |
| RMSRE(MLE) | 0.072 | 0.072 | 0.072 | 0.072 | 0.073 | 0.076 |
| Extrapolate to $t = 2, \psi(1) = 1000$ | | | | | | |
| b | 0.01 | 0.02 | 0.03 | 0.05 | 0.1 | 0.2 |
| RMSRE(Curve-fitting) | 0.033 | 0.034 | 0.036 | 0.043 | 0.065 | 0.106 |
| RMSRE(MLE) | 0.032 | 0.032 | 0.032 | 0.033 | 0.033 | 0.034 |
| Extrapolate to $t = 4, \psi(1) = 200$ | | | | | | |
| b | 0.01 | 0.02 | 0.03 | 0.05 | 0.1 | 0.2 |
| RMSRE(Curve-fitting) | 0.074 | 0.075 | 0.077 | 0.084 | 0.110 | 0.166 |
| RMSRE(MLE) | 0.073 | 0.074 | 0.074 | 0.076 | 0.079 | 0.086 |
| Extrapolate to $t = 4, \psi(1) = 1000$ | | | | | | |
| b | 0.01 | 0.02 | 0.03 | 0.05 | 0.1 | 0.2 |
| RMSRE(Curve-fitting) | 0.034 | 0.037 | 0.042 | 0.055 | 0.091 | 0.155 |
| RMSRE(MLE) | 0.033 | 0.033 | 0.034 | 0.034 | 0.035 | 0.038 |

Table D. Simulation results for geometric distribution

| Extrapolate to $t = 2$, $\psi(1) = 200$ | | | | | | |
|---|-------|-------|-------|-------|-------|-------|
| b | 0.05 | 0.1 | 0.2 | 0.4 | 0.6 | 0.8 |
| RMSRE(Curve-fitting) | 0.322 | 0.458 | 0.587 | 0.687 | 0.731 | 0.756 |
| RMSRE(MLE) | 0.085 | 0.106 | 0.136 | 0.165 | 0.174 | 0.174 |
| Extrapolate to $t = 2$, $\psi(1) = 1000$ | | | | | | |
| b | 0.05 | 0.1 | 0.2 | 0.4 | 0.6 | 0.8 |
| RMSRE(Curve-fitting) | 0.316 | 0.454 | 0.583 | 0.684 | 0.728 | 0.753 |
| RMSRE(MLE) | 0.054 | 0.079 | 0.111 | 0.134 | 0.136 | 0.132 |
| Extrapolate to $t = 4$, $\psi(1) = 200$ | | | | | | |
| b | 0.05 | 0.1 | 0.2 | 0.4 | 0.6 | 0.8 |
| RMSRE(Curve-fitting) | 0.320 | 0.462 | 0.601 | 0.716 | 0.768 | 0.798 |
| RMSRE(MLE) | 0.102 | 0.145 | 0.218 | 0.311 | 0.366 | 0.397 |
| Extrapolate to $t = 4$, $\psi(1) = 1000$ | | | | | | |
| b | 0.05 | 0.1 | 0.2 | 0.4 | 0.6 | 0.8 |
| RMSRE(Curve-fitting) | 0.315 | 0.458 | 0.598 | 0.713 | 0.766 | 0.796 |
| RMSRE(MLE) | 0.075 | 0.122 | 0.188 | 0.254 | 0.279 | 0.287 |